

## Excitation of giant resonances in $^{28}\text{Si}$ with 250 MeV protons

J. Lisantti,\* F. E. Bertrand, D. J. Horen, B. L. Burks, and C. W. Glover  
Oak Ridge National Laboratory, Oak Ridge, Tennessee 37831

D. K. McDaniels

University of Oregon, Eugene, Oregon 97403

L. W. Swenson and X. Y. Chen

Oregon State University, Corvallis, Oregon 97330

O. Häusser

Simon Fraser University, Burnaby, British Columbia, Canada V5A 1S6

K. Hicks

TRIUMF, Vancouver, British Columbia, Canada V6T 2A3

(Received 21 January 1988)

Differential cross section measurements have been made for 250 MeV proton inelastic scattering from  $^{28}\text{Si}$ . Hadronic deformation lengths for the states at 1.78 ( $2^+$ ), 4.62 ( $4^+$ ), 6.8 ( $3^-$  and  $4^+$ ), 9.70 ( $5^-$ ), and 10.2 MeV ( $3^-$ ) have been extracted using a first-order vibration model distorted-wave Born approximation description. Deformation lengths for the  $2^+$  and  $4^+$  states are found to be independent of proton energy from 40 to 500 MeV. Cross sections for the excitation of the giant resonance region are found to be highly fragmented between 16 to 25 MeV. This region of excitation is found to contain an energy weighted sum rule depletion of 70% for the isovector giant dipole resonance, 26% for the isoscalar giant quadrupole resonance, and 5% for the isoscalar hexadecapole resonance. No structure was observed in the inelastic continuum region of 25 to 45 MeV of excitation energy.

### I. INTRODUCTION

Giant resonance studies with intermediate energy protons have mainly concentrated on nuclei with  $A \geq 40$ .<sup>1-10</sup> In such nuclei the excitation energy region near  $63 A^{-1/3}$  MeV is generally dominated by a single large structure, containing the isoscalar ( $\Delta T=0$ ) giant quadrupole resonance (ISGQR), the isoscalar giant hexadecapole resonance (ISGHR), and the isovector ( $\Delta T=1$ ) giant dipole resonance (IVGDR) which is nearly degenerate in energy with the isoscalar giant monopole resonance (ISGMR). In order to understand this region of excitation energy, it is necessary to utilize results from the investigations with several different probes in order to decompose the complicated giant resonance (GR) spectrum. Photonuclear measurements clearly define the excitation energy, width, and sum rule depletion of the IVGDR, while inelastic alpha scattering selectively excites the ISGQR and ISGMR. For the higher multipole GR's the selectivity of intermediate energy protons to identify the various angular momentum transfers is needed.<sup>4-11</sup> Utilization of such a variety of probes has led to a good understanding of the GR region in heavier nuclei.

In lighter nuclei the giant resonance strength is found to be highly fragmented. Consequently, identifying the various GR's in lighter nuclei is much more difficult. This has resulted in substantial disagreement between various studies.

Early inelastic scattering studies of the GR region in  $^{28}\text{Si}$  with incident protons of 61 MeV suggested that no more than 30% of the ISGQR energy weighted sum rule (EWSR) was depleted, with the IVGDR exhausting  $\sim 40\%$  of its sum rule.<sup>12</sup> A reanalysis<sup>13</sup> of this data which included a comparison with 120 MeV ( $\alpha, \alpha'$ ) data concluded that the GR region contained little IVGDR strength excited by ( $p, p'$ ) but instead contained ISGMR strength. This conclusion was based upon the premise that the ( $p, p'$ ) data should contain both isovector and isoscalar strength while the ( $\alpha, \alpha'$ ) data should only contain isoscalar strength. Differences between the spectra would then be attributable to isovector excitations. The fact that there was essentially no difference between the ( $p, p'$ ) and the ( $\alpha, \alpha'$ ) spectra led to authors of Ref. 13 to conclude that the region contained little IVGDR strength which was excited by inelastic proton scattering.

A study of the ( $n, p$ ) reaction<sup>14</sup> performed at 59.6 MeV reported a broad structure in the continuum near 20 MeV of excitation energy. The angular distribution for this peak could be described by an  $L=1$  angular momentum transfer. Hence, it was identified as the analog of the IVGDR in  $^{28}\text{Si}$ , which exhausted  $88 \pm 18\%$  of the EWSR.

A study using 129 MeV alpha particle inelastic scattering on targets ranging from  $^{12}\text{C}$  to  $^{208}\text{Pb}$  and angles of  $0^\circ \leq \theta_L \leq 8^\circ$ , showed no evidence for the excitation of the ISGMR in nuclei with  $A \leq 58$ .<sup>15</sup> Another group using 120 MeV alpha particles reported<sup>16</sup> a sum rule depletion

of 4.5% for the ISGMR in  $^{28}\text{Si}$ , in the region of 14–25 MeV. In the latter experiment the smallest scattering angle attainable was  $6^\circ$ , which severely limited their ability to distinguish between the ISGMR and ISGQR. In a recent  $(\alpha, \alpha')$  study at 129 MeV it was reported<sup>17</sup> that  $66 \pm 20\%$  of the EWSR for the ISGMR was depleted in a region centered at 17.9 MeV with a width of 4.8 MeV.

An experiment using 115 MeV protons<sup>5</sup> reported that the GR region contained both IVGDR and ISGMR strength. In this analysis, the IVGDR strength was fixed at 60% of the EWSR in accordance with photonuclear studies. In fitting the cross section for the region of 15.7–24.1 MeV a sum of angular momentum transfers of  $L=0, 1, 2,$  and  $4$  was used. This work reported  $34 \pm 13\%$  of the EWSR for the ISGMR in the region noted. In summary, the relative strengths of the ISGMR and IVGDR in  $^{28}\text{Si}$  are not well established.

The magnitude and, to a lesser extent, the shape of the angular distribution for the IVGDR excited in the  $(p, p')$  reaction are sensitive to the strength of the isovector potential  $V_\tau$ . The correct value of  $V_\tau$  to be used is not well established. Values ranging from 2 to 25 MeV have been used in the analysis<sup>8</sup> of the excitation of the IVGDR in inelastic proton scattering.

There is considerably better agreement on the location and strength of the ISGQR. The strength is found to be distributed over an excitation region of 16–24 MeV. Different experiments<sup>5,16,17</sup> yield an EWSR depletion between 19 and 34%. Variations of the reported strength of the ISGQR may arise from difficulties in establishing the strengths of the ISGMR and IVGDR excitations.

There is little information pertaining to giant resonance strength with multipolarity higher than two in  $sd$ -shell nuclei. The  $3\hbar\omega$   $L=3$  giant octupole resonance (ISGOR) has been observed in many nuclei for  $A \geq 40$ .<sup>2,3,6,8,10</sup> As is the case for the ISGQR in  $^{28}\text{Si}$  the ISGOR may also be fragmented. However, being a  $3\hbar\omega$  excitation the ISGOR would likely be located at a higher excitation energy than the IVGDR, ISGMR, and ISGQR. No evidence for this higher lying  $L=3$  resonance in  $^{28}\text{Si}$  was found in the previous  $(\alpha, \alpha')$  and  $(p, p')$  experiments. The excitation of the  $2\hbar\omega$  isoscalar giant hexadecapole resonance (ISGHR) has been directly observed in  $^{208,206}\text{Pb}$  (Refs. 6, 8, and 10) and is expected to be present in other nuclei. Being a  $2\hbar\omega$  excitation, the ISGHR is expected to be nearly degenerate in energy with the ISGQR. Intermediate energy protons with their excellent selectivity to angular momentum transfer have proven to be good probes in also searching for high multipolarity giant resonances. This can be seen from Fig. 1 which shows the angular distributions for  $L=0-5$  natural parity states in  $^{28}\text{Si}$  which exhaust 100% of their EWSR. Except for  $L=0$ , the first maximum for each distribution provides a unique signature for each momentum transfer. This is not the case for most other probes. An interesting feature to be noted in Fig. 1 is the magnitude of the cross section for the ISGMR. Like the IVGDR, the angular distribution of the ISGMR (as calculated in "version I" of Satchler) is peaked at smaller scattering angles. However, its cross section at small angles is only about 15% of the IVGDR, hence, with com-

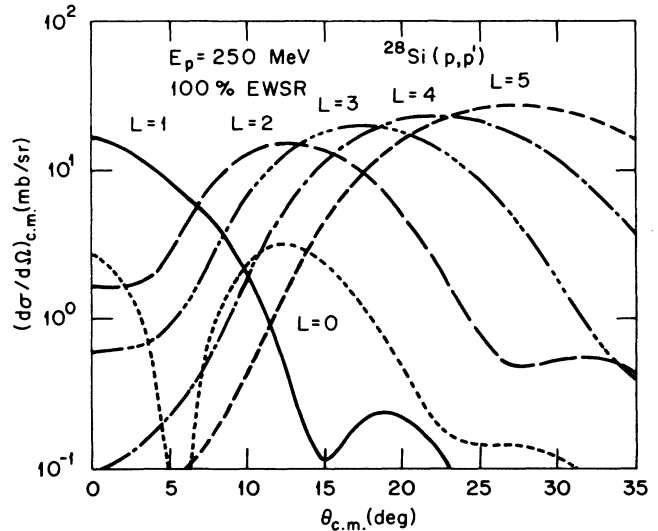


FIG. 1. Angular distribution for the  $L=0-5$  giant resonances exhausting 100% of their EWSR in  $^{28}\text{Si}$  excited by 250 MeV protons.

parable EWSR depletions, it would be difficult to distinguish the ISGMR from the IVGDR. Furthermore, the second diffraction maximum for the ISGMR occurs at the same angle as the first maximum of the ISGQR and in this angle range the  $L=2$  cross section is nearly a factor of ten larger than that for  $L=0$  (both for 100% EWSR depletion). For these reasons inelastic scattering of intermediate energy protons is not an appropriate reaction to use to uniquely identify the ISGMR strength distribution.

We also report on elastic scattering and the inelastic excitation of low-lying collective states, an extension of work we have previously reported for  $^{208}\text{Pb}$  (Refs. 18 and 19) and  $^{40}\text{Ca}$ .<sup>20</sup> In our previous works it was shown that the hadronic deformation length  $\delta_H = \beta_L R$  extracted in a collective model distorted-wave Born approximation (DWBA) analysis was independent of the incident proton energy up to 800 MeV, in agreement with results for  $^{12}\text{C}$ ,<sup>21</sup> and  $^{116,124}\text{Sn}$ .<sup>22</sup> The fact that deformation lengths are constant with energy allows the extraction of precise ratios of neutron to proton multipole matrix elements  $M_n/M_p$  using the average deformation length. Accurate values of  $M_n/M_p$  are important for nuclear structure calculations.<sup>23</sup>

## II. EXPERIMENT

The experiment was performed at TRIUMF (Tri-Universities Meson Facility) using the upgraded Medium Resolution Spectrometer Facility (MRS). The incident proton beam had an energy of 250 MeV and the intensity varied from 0.1 to 2 nA depending upon the spectrometer angle setting. The beam current was measured using a Faraday cup located inside the scattering chamber. The target was made of natural silicon and had a thickness of  $36.3 \text{ mg/cm}^2$ . The MRS has been described in detail elsewhere.<sup>8,19</sup>

Measurements for the excitation of the giant resonance region were made at laboratory angles of 6, 10, 13, 17, 21, and 25 degrees. An overall energy resolution of  $\sim 150$  keV (FWHM) was obtained at all angles.

Two checks of the absolute cross section normalizations were made. The elastic scattering cross sections were compared with those from another recent study of elastic scattering on  $^{28}\text{Si}$  at 200, 250, and 400 MeV.<sup>24</sup> Results from the two measurements were found to agree within  $\pm 10\%$ , after applying an angle shift correction of  $0.25^\circ$  to the present experiment. We have also measured elastic proton scattering from a  $\text{CH}_2$  target at angles of 10, 13, 17, and 21 deg. Our measured cross sections for elastic scattering from hydrogen agree with calculations using a phase shift parametrization<sup>25</sup> to within  $\pm 8\%$ . We assign an uncertainty of 10% to our absolute normalization.

### III. DATA AND RESULTS

#### A. Elastic and low-lying collective states

Hadronic deformation lengths obtained in the collective model DWBA analysis are sensitive to the values of the optical model parameters (OMP) that are used.<sup>10</sup> Thus, precise and extensive elastic scattering cross sections and analyzing power  $[A_y(\theta)]$  data are needed. In the present experiment, elastic cross sections data to  $42^\circ$  were obtained. Since the data of Ref. 24 are more extensive than ours in that they also contain analyzing powers, they were fitted in order to deduce optical model parameters. These parameters were then used as a starting point in fitting our data. Only minor changes to the imaginary and real spin-orbit radii were needed in order to fit our elastic scattering data. Figure 2 shows the fit to our elastic scattering angular distribution obtained using the code ECIS79 (Ref. 26) and the deduced parameters are listed in Table I.

Measured angular distributions for some of the well known low-lying collective states in  $^{28}\text{Si}$  are shown in Fig. 3. The solid curves show calculations using the OMP tabulated in Table I. Good comparisons between the

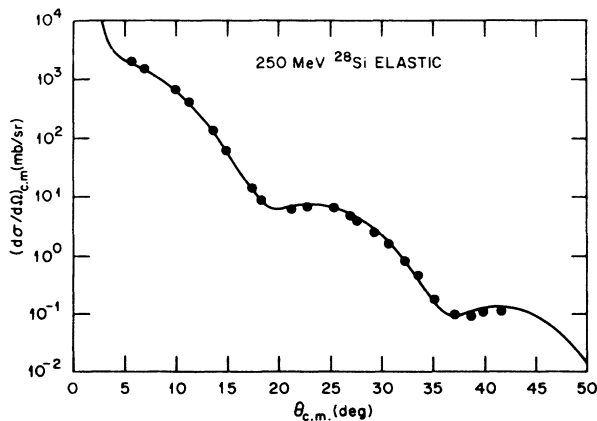


FIG. 2. Differential cross section for the elastic scattering of 250 MeV protons from  $^{28}\text{Si}$ . The curve is an optical model fit using ECIS79 with parameters from Table I.

TABLE I. Optical model parameters for 250 MeV  $^{28}\text{Si}(p,p)$  elastic scattering.

$V_R = 8.081$ MeV
$r_R = 1.373$ fm
$a_R = 0.741$ fm
$V_I = 26.853$ MeV
$r_I = 1.05$ fm
$a_I = 0.664$ fm
$V_{\text{RSO}} = 3.668$ MeV
$r_{\text{RSO}} = 0.900$ fm
$a_{\text{RSO}} = 0.595$ fm
$V_{\text{ISO}} = -3.660$ MeV
$r_{\text{ISO}} = 0.929$ fm
$a_{\text{ISO}} = 0.623$ fm
$r_c = 1.2$ fm

data and calculations are obtained for the five angular distributions shown.

In a collective vibrational model the only normalization parameter is the hadronic deformation length; the cross sections scale as  $(\delta_H)^2$ . A first order vibrational model was used to analyze these states since it will be the model applied in the analysis of the giant resonances. All calculations were performed with ECIS79, and the five deformation lengths of the transition potential ( $\beta_L R_R$ ,  $\beta_L R_I$ ,  $\beta_L R_{\text{RSO}}$ ,  $\beta_L R_{\text{ISO}}$ ,  $\beta_L R_C$ , where RSO and ISO are the real and imaginary spin orbit terms) were set equal to each other. For each calculated angular distribution on Fig. 3 the hadronic deformation length  $\delta_H = \beta_L R$  used to normalize the calculation is given.

In the analysis of the peak observed at 6.8 MeV we utilized the fact that there is a well known  $3^-$ ,  $4^+$  doublet at 6.878 and 6.888 MeV, respectively. Since these states could not be resolved experimentally, their calculated cross sections were added incoherently and the deformation lengths adjusted to give a “best fit” to the data.

In our collective model analysis, the reduced transition probabilities  $B(EL)\uparrow$ 's were calculated from the extracted hadronic deformation lengths,  $\delta_H$ . For a transition which is of a “pure” isoscalar character one can relate the  $B(EL)\uparrow$  to the  $\delta_H$  by the relation

$$B(EL)\uparrow = \left( \frac{3Z}{4\pi} \right)^2 (\delta_H)^2 R^{2L-2}, \quad (1)$$

where a uniform charge distribution is assumed. We take the radius  $R$  to be  $R = 1.2 A^{1/3}$ . This  $B(EL)\uparrow$  can then be compared with values from electromagnetic data.

For the  $2^+$ , 1.78 MeV state we obtain  $\delta_H = 1.18 \pm 0.12$  fm which corresponds to  $B(E2)\uparrow = 206 \pm 45 e^2 \text{fm}^4$ . This can be compared with the value from electron scattering of  $B(E2)\uparrow = 337 \pm 30 e^2 \text{fm}^4$ .<sup>27</sup> We have done an independent fit to the angular distributions for the  $2^+$  state at proton energies of 135, 250, and 500 MeV using ECIS79 in order to ensure a consistent analysis across this energy range. Plotted on Fig. 4 are values of the hadronic deformation lengths determined from proton inelastic scattering measurements for the  $2^+$ , 1.78 MeV, and  $4^+$ , 4.62 MeV states.<sup>28</sup> Within the uncertainties, the data suggest

that the deformation lengths for the  $2^+$  and  $4^+$  states are independent of incident proton energy except for the 115 MeV point for the  $2^+$  state. This is in good agreement with similar findings reported in earlier works.<sup>18-22</sup> The average for the  $2^+$  state excluding the 115 MeV point is  $\delta_H = 1.26 \pm 0.08$  fm which yields  $B(E2)\uparrow = 235 \pm 31$

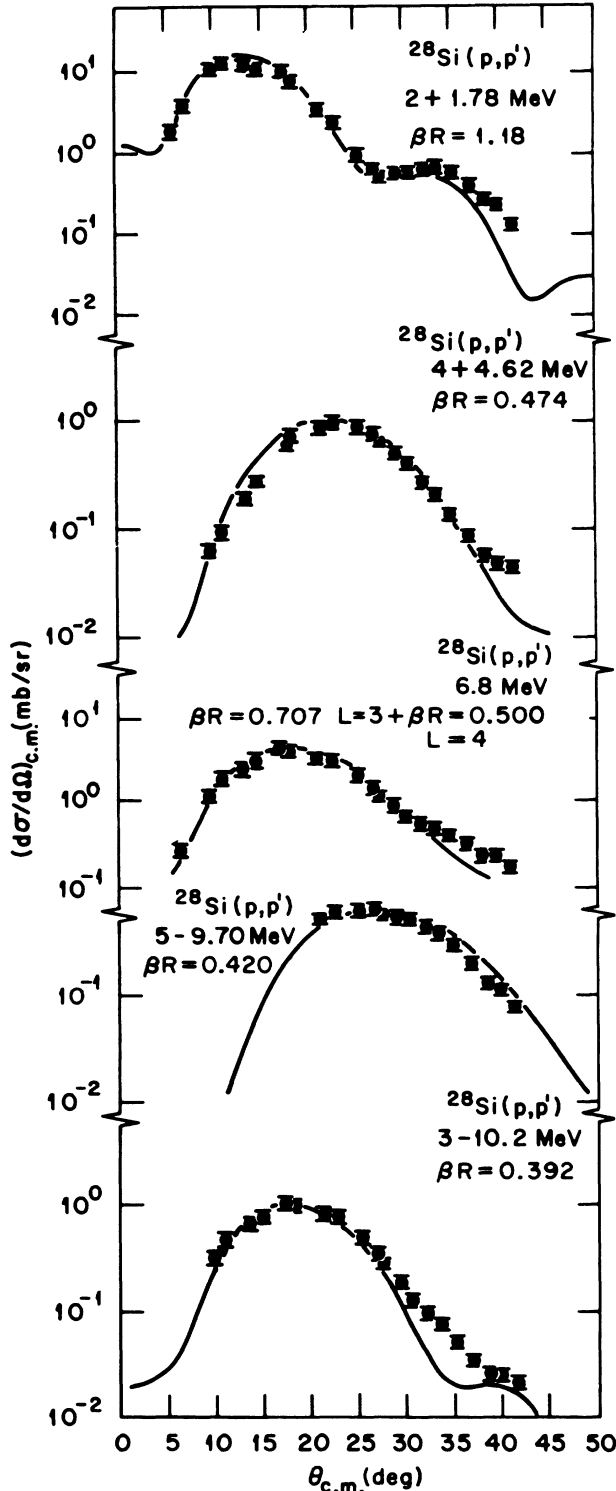


FIG. 3. Differential cross sections for various states in  $^{28}\text{Si}$ . The deformation lengths extracted are shown for each state, the dimensions are in fermis.

$e^2\text{fm}^4$ . This is significantly lower than the  $B(E2)\uparrow$  value reported from electron scattering.

The deformation lengths can be related to multipole matrix elements.<sup>23</sup> The multipole matrix element is defined as

$$M_{p,n}(\lambda) = \int_0^\infty \rho_{tr}^{p,n}(r) r^{\lambda+2} dr, \quad (2)$$

where  $\rho_{tr}^{p,n}(r)$  is the transition density for protons, neutrons, and  $\lambda$  is the angular momentum transfer. In the collective model the transition density is given by

$$\rho_{tr}^{p,n}(r) = \delta_{p,n} \frac{\partial U_{opt}}{\partial r}, \quad (3)$$

which leads to<sup>19</sup>

$$\begin{aligned} \frac{M_n}{M_p} &= \left[ \frac{N}{Z} \right] \left[ \frac{\delta_n}{\delta_p} \right] \\ &= \left[ \frac{N}{Z} \right] \left[ \frac{\delta_H}{\delta_p} + \frac{Z}{b_n^p/b_p^p N} \left[ \frac{\delta_H}{\delta_p} - 1 \right] \right]. \end{aligned} \quad (4)$$

where  $(b_n^p/b_p^p)$  is the ratio of the neutron to proton force.<sup>23</sup> The parameter  $\delta_p$  is the electromagnetic deformation length deduced from the expression:

$$\delta_p^2 = \left[ \frac{4\pi}{Z(\lambda+2)} \right]^2 B(EL)\uparrow \frac{1}{\langle r^{\lambda-1} \rangle^2}, \quad (5)$$

where the moments  $\langle r^{\lambda-1} \rangle$  come from charge distributions<sup>29</sup> and the  $B(EL)\uparrow$  is from electron scattering. From Eq. (4), it is seen that  $\delta_H \neq \delta_p$  implies  $M_n/M_p$  does not equal the collective value  $(N/Z)$  which means that  $\delta_n \neq \delta_p$ . Using Eq. (4) with a neutron to proton force ratio of one, we find for the  $2^+$  state that  $M_n/M_p = 0.85 \pm 0.09(N/Z)$ , for  $\delta_H = 1.26 \pm 0.08$  fm, and  $\delta_p = 1.36 \pm 0.05$  fm. This implies that for the  $2^+$  state the transition densities for the neutrons and protons are different. However,  $\pi^+/\pi^-$  inelastic scattering data which can also be used to determine  $M_n/M_p$  leads to quite a different conclusion. With 162 MeV pions Olmer *et al.*<sup>30</sup> found  $\delta_H = 1.49 \pm 0.06$  fm ( $\pi^+$ ) and

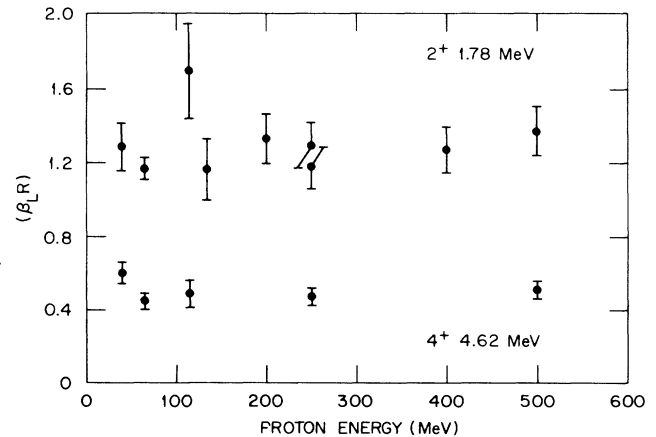


FIG. 4. Values for the deformation lengths extracted for the  $2^+$  1.78 and  $4^+$  4.62 MeV states as a function of incident proton energy. The references for each energy is given in Ref. 28.

$\delta_H = 1.47 \pm 0.06$  fm ( $\pi^-$ ) for the  $2^+$  1.78 MeV state, when the data were analyzed using an impulse approximation with the same transition density as used here in the proton analysis. Their result implies  $M_n/M_p = (N/Z)$ . In taking into account the uncertainty in both  $\pi^+$  and  $\pi^-$  measurements there is a marginal agreement between the proton data and the results of Ref. 30. From scattering with 50 MeV pions, Wienands *et al.*<sup>31</sup> found  $M_n/M_p = 1.13 \pm 0.09$ . Clearly there is a discrepancy between the proton and the lower energy pion results. Experiments with other probes, ranging from alphas to  $^{16}\text{O}$ ,<sup>16,32</sup> yield deformation lengths which are in excellent agreement with that found in proton scattering.

### B. Giant resonance region

Data shown in Fig. 5 were obtained on  $^{28}\text{Si}$  at six angles covering an excitation energy up to 45 MeV. In previous studies<sup>5,12,16,17</sup> of this nucleus the giant resonance region has been defined as starting near 15 MeV and continuing upward in excitation energy. All of the previous experiments covered an excitation region extending up to 30–35 MeV. Our results confirm earlier studies which found no significant structure beyond 25 MeV. Figure 5 shows that the GR region exhibits considerable structure which changes from angle to angle indicating the presence of several multiplicities. Similar structure of the GR region has been observed in all nuclei studied with  $A \leq 40$ .<sup>33</sup>

A particular concern in all giant resonance studies is how to define the continuum which underlies the reso-

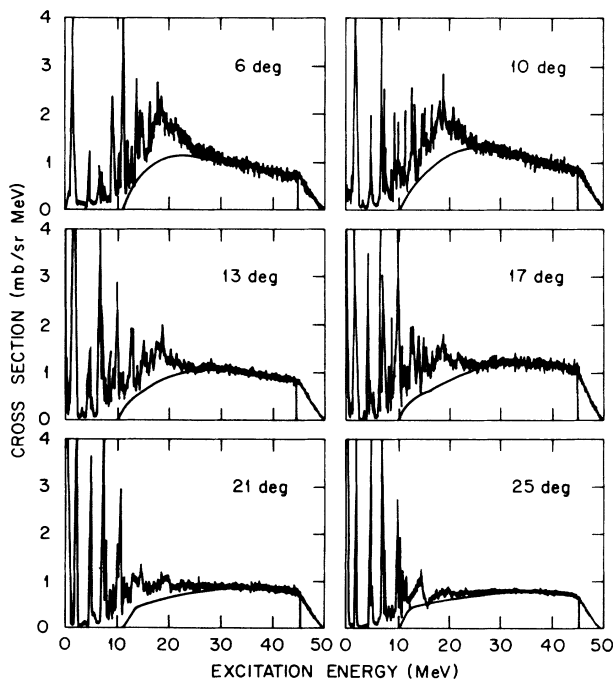


FIG. 5. Spectra for all of the angles studied which used the full momentum acceptance of the MRS. The curve drawn for each angle comes from the phenomenological model for quasifree scattering as mentioned in the text.

nance region. Considerable progress has been made in trying to understand the reaction mechanisms that are responsible for the inelastic continuum. One suggestion is that the continuum arises from quasifree single step nucleon-nucleon scattering.<sup>8,34,35</sup> In Refs. 8 and 34 a completely phenomenological approach was used in order to describe this quasifree process. The continuum was fitted with a function of the form

$$N(E) = N_0 e^{-(E-E_0)^2/\lambda} (1 - e^{-\alpha E}), \quad (6)$$

for excitations at and below that of the quasifree peak. The parameter  $N_0$  is the maximum height in cross section for a Gaussian whose centroid  $E_0$  is determined as that point where the slope of the continuum is zero. The parameter  $\lambda$  which is used to simulate the Fermi motion of the struck nucleons<sup>8</sup> is interpreted as the width of the Gaussian and is determined so that the curve fits the data at each angle. The parameter  $\alpha$  is a cutoff factor applied so that the continuum curve will go to zero at a predetermined excitation energy, usually the neutron separation energy. For excitation energies above that for quasifree scattering Eq. (6) is connected to a fourth order polynomial. The use of this formalism to simulate the continuum shape and magnitude has been supported by recent Monte Carlo calculations.<sup>36</sup>

The above phenomenological procedure was used to draw the curves through the data in Fig. 5. Attempts were also made to fit the continuum using the free response of a semi-infinite slab approach of Bertsch, Scholten, and Esbensen.<sup>37,38</sup> This model was unable to reproduce the continuum part of the spectra especially for the 6 and 10 deg data. The calculated continuum shape was shifted to lower excitation energies than the data. A similar lack of agreement was also found with the relativistic continuum model of Horowitz and Iqbal<sup>39</sup> which uses a Fermi gas model for the nuclear response.

The phenomenological curve for the nuclear continuum as shown in Fig. 5, was subtracted from the data, leaving what we define as the giant resonance cross section. Spectra resulting from the subtraction are shown in Fig. 6 for the excitation energies of 16–26 MeV.

The spectra in Fig. 6 have been integrated over excitation energy bins of varying widths that contain various structures. Cross sections were obtained for nine different excitation energy regions as shown in Fig. 6. These regions are 16.0–16.87, 16.87–17.46, 17.46–18.48, 18.48–19.44, 19.44–20.30, 20.30–21.0, 21.0–22.64, 22.64–23.52, and 23.52–25.0 MeV. Also, the region of 16.0–25.0 MeV was integrated in order to help deduce the multiplicities and sum rule strengths contained in the entire GR region. The angular distribution for the entire GR region is shown in Fig. 7. The background subtraction procedure is mainly responsible for the uncertainty of 20–30%. In fitting the data of Fig. 7 a minimum number of multipoles was used. In all searches  $L=1$  and  $L=2$  were included. This was done since all previous studies have found a sum rule fraction of at least 19% for the ISGQR and results of photonuclear measurements<sup>40</sup> clearly show IVGDR strength in this excitation energy region of  $^{28}\text{Si}$ . As previously noted, the ISGMR strength is predicted to be considerably less

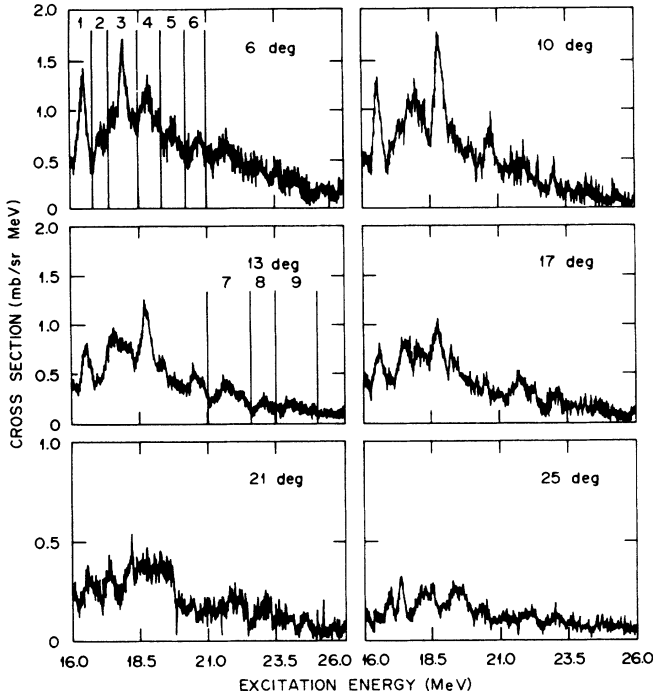


FIG. 6. Spectra in which the continuum curves of Fig. 4 have been subtracted from the data. Note the change of scale for the 21° and 25° spectra.

than that for the IVGDR and ISGQR. For this reason we have chosen not to include any  $L=0$  strength in our analysis.

Various combinations of  $L=1+2+4$  and  $L=1+2+3$  were tried with a reasonable fit for the entire GR region obtained with  $L=1$  (70%) + 2 (26%) + 4 (5%) where the  $L=1$  EWSR is fixed from photonuclear work.<sup>40</sup> The lack of agreement for the 6 deg point is discussed later in this section. From Figs. 6 and 7 it can be seen that higher multipoles of either  $L=3$  or 4 are needed since there is considerable cross section in both the 21 and 25 degree data, and Fig. 1 shows that only the higher multipoles can contribute at the larger angles. Our best fit favors the  $L=4$  over the  $L=3$  assignment. This is con-

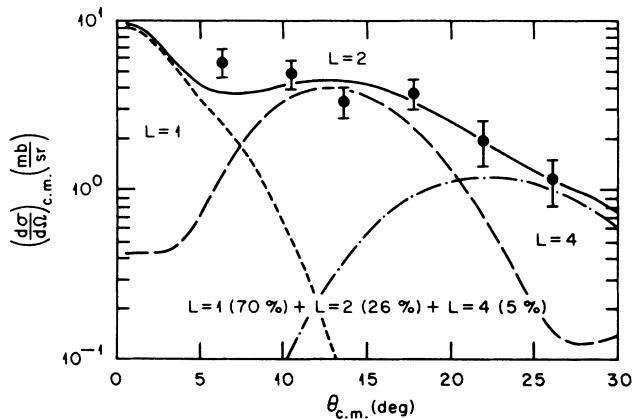


FIG. 7. Differential cross section for the summed region of 16.0–25 MeV, along with sum rule depletions for  $L=1, 2,$  and 4.

sistent with results from the 120 MeV ( $\alpha, \alpha'$ ) measurements of Ref. 16 where negligible  $L=3$  strength was observed in the GR region. Inelastic alpha scattering should be sensitive to this  $L=3$  strength since the differential cross sections for even and odd multipoles oscillate out of phase with one another.

Since the best fit to the angular distribution for the region of 16–25 MeV was obtained with a combination of  $L=1, 2,$  and 4, these three multipoles were then used in fitting the various integrated regions. These results are shown in Fig. 8. As a starting point in fitting the nine regions the EWSR strength of the IVGDR was fixed from the photonuclear work of Ref. 40. The ISGQR and ISGHR strengths were then allowed to vary in order to achieve the best fit. This gives a result for the sum of the EWSR depletion for the ISGQR that is slightly different than that given in Fig. 7. As Fig. 7 shows, for the region of 16–25 MeV the percent EWSR for the ISGQR is 26%, and from the addition of the nine regions it is 30%. These differences indicate the uncertainties in determining EWSR strengths from ( $p, p'$ ) data. From the shape of the angular distributions for the various multipoles it can be seen that for each of the nine angular distributions of Fig. 8 no one multipolarity would fit the data. Instead various strength combinations of  $L=1, 2,$  and 4 are needed. Each angular distribution shows the EWSR depletion associated with each multipolarity required to fit the data. These values are also tabulated in Table II.

In Fig. 9 the 6 deg spectrum from our measurements is plotted and compared with the photonuclear measurements of Ref. 40. The 6 deg data were chosen since in the ( $p, p'$ ) reaction the cross section from Coulomb excitation causes the IVGDR to peak at small angles, and therefore, there should be minimal contributions from higher multipoles. To illustrate this, the cross section for the ISGQR is histogrammed on Fig. 9. The photonuclear spectrum was normalized to match the ( $p, p'$ ) spectrum at 19.5 MeV. For the region of 19.5 MeV and above, the sum of the photonuclear and the ISGQR is slightly above the data implying that the normalization of the photonuclear cross section to match the data at 19.5 MeV is a reasonable approximation, and at worst would serve as an upper limit for the IVGDR cross section. Assuming a sum rule depletion of 10.5% for the IVGDR for the 19.44–20.30 MeV region the value of the isovector potential  $V_\tau$  was adjusted so that the IVGDR calculation reproduced the 6 deg cross section along with a small contribution from the ISGQR. A value of 4.5 MeV for  $V_\tau$  gave the best fit to the data. As was mentioned above, this may represent an upper limit on  $V_\tau$ . We use this value of  $V_\tau$  along with the sum rule depletions found from the photonuclear work for all further IVGDR calculations. Reasonable variations of the value of  $V_\tau$  do not affect the sum rules found for the ISGQR or ISGHR since the angular distribution of the IVGDR falls off rapidly with angle.

Figure 9 shows an interesting result for the excitation energies below 19.5 MeV. The sum of the photonuclear cross section and the ISGQR cross section yields a value that is much lower than the data. Recent analysis<sup>41</sup> of giant resonance data on  $^{40}\text{Ca}$  using 500 MeV protons shows

that the region of excitation energy below the IVGDR contains excitation of the isovector spin-flip giant dipole resonance ( $\Delta L=1, \Delta S=1, J^\pi=0^-, 1^-, 2^-$ ). One indication of this resonance is that for the angles studied in  $^{40}\text{Ca}$  the spin-flip giant dipole has a flat angular distribution in  $(p, p')$  scattering at 500 MeV for angles from approximately 3–8 deg. Spin-flip strength can also be identified by measurement of the spin-flip cross section  $\sigma S_{\text{NN}}$  in  $(\bar{p}, \bar{p}')$  studies. Sawafra *et al.*<sup>42</sup> have done such a study at 250 MeV on  $^{24}\text{Mg}$  at scattering angles of 2.9 and 6.6 degrees. They consistently observed structure in the  $\sigma S_{\text{NN}}$  spectra in the region of 15–25 MeV, implying

the existence of spin-flip strength in our region of interest.

#### IV. DISCUSSION

Data have been obtained in  $^{28}\text{Si}$  covering the region of the ground state up to 45 MeV of excitation energy for proton scattering from 6–41 deg in the lab. Optical model parameters were derived from fits to elastic scattering data, which were then used in first order vibrational model calculations for low lying collective states and for excitations in the giant resonance region.

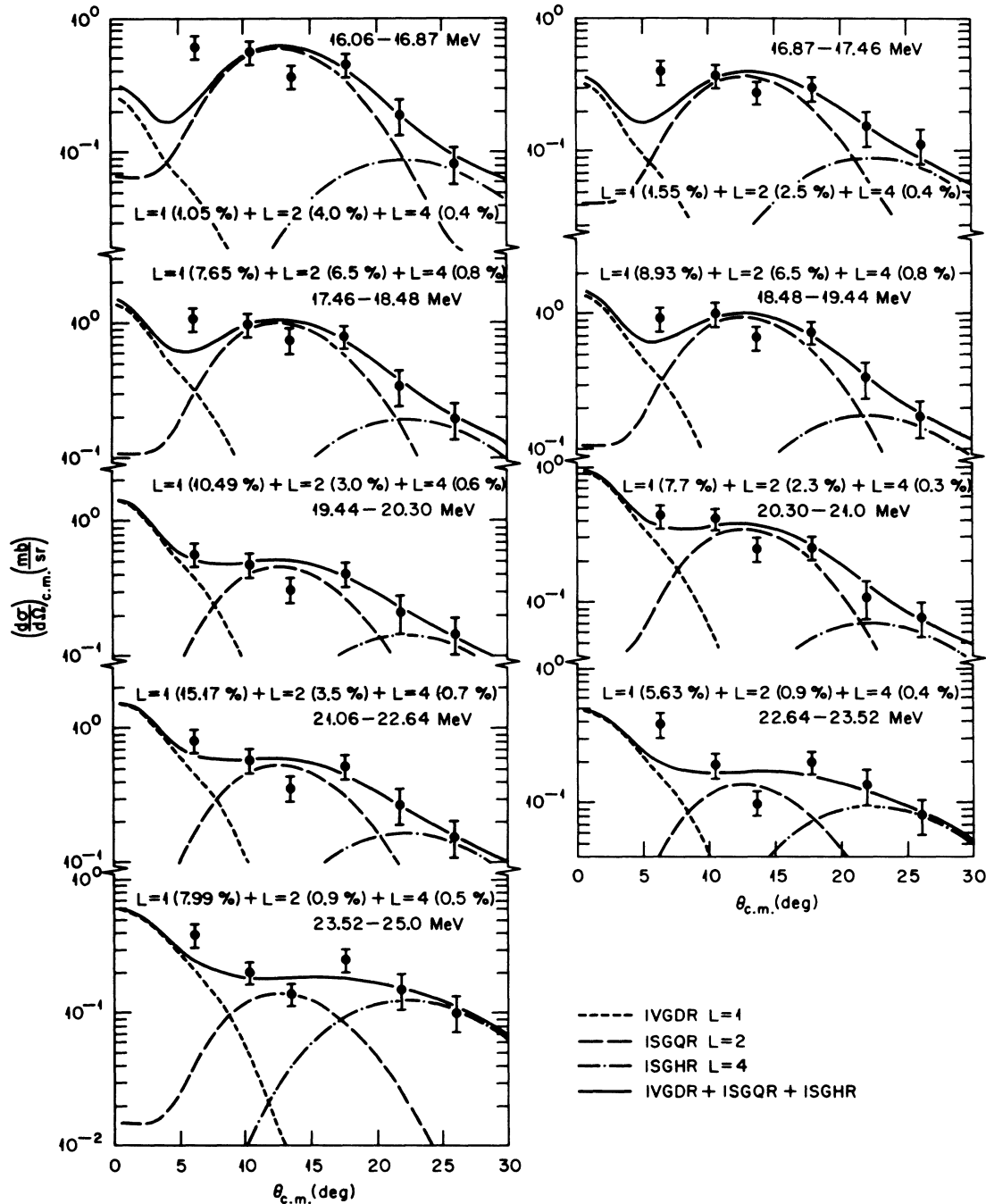


FIG. 8. Differential cross sections for the nine regions of 16.06–25 MeV, along with the sum rule depletions.

TABLE II. Energy weighted sum rule (EWSR) depletions for the IVGDR, ISGQR, and ISGHR for the nine spectra regions.

$E_x$ (MeV)	EWSR (%) IVGDR	EWSR (%) ISGQR	EWSR (%) ISGHR
16.00 <sup>-</sup>	1.05	4.0	0.4
16.87			
16.87 <sup>-</sup>	1.55	2.5	0.4
17.46			
17.46 <sup>-</sup>	7.65	6.5	0.8
18.48			
18.48 <sup>-</sup>	8.93	6.5	0.8
19.44			
19.44 <sup>-</sup>	10.49	3.0	0.6
20.30			
20.30 <sup>-</sup>	7.8	2.3	0.3
21.0			
21.0 <sup>-</sup>	15.17	3.5	0.7
22.64			
22.64 <sup>-</sup>	5.63	0.9	0.4
23.52			
23.52 <sup>-</sup>	7.99	0.9	0.5
25.0			

The DWBA calculations for known low lying states, shown in Fig. 3, reproduce the shapes of the angular distributions for angular momenta and parities of  $2^+$ ,  $3^-$ ,  $4^+$ , and  $5^-$ . The hadronic deformation lengths,  $\delta_H = \beta R$ , extracted for the 1.78  $2^+$ , and 4.62 MeV  $4^+$  states agree with other proton results for incident beam energies of 40–500 MeV, thus supporting other recent results<sup>18–22</sup> which show that the collective model DWBA provides a

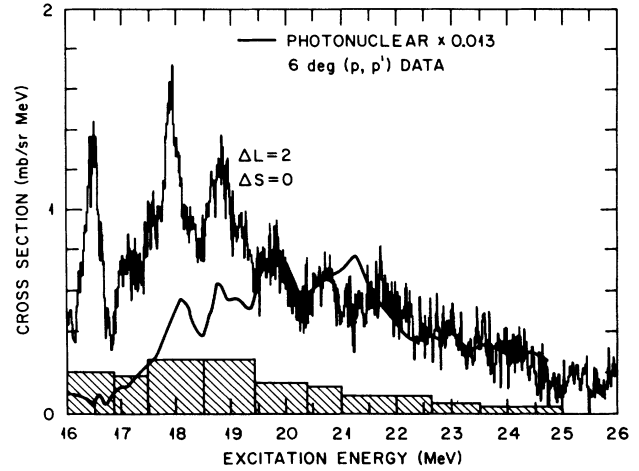


FIG. 9. Photonuclear cross section from Ref. 40 compared to a 250 MeV (p,p') spectra taken at 6 deg. The photonuclear data were normalized to match the (p,p') data at 19.5 MeV. Note that the photonuclear data are a total cross section. The hatched histogram is the cross section for the ISGQR.

good description of inelastic scattering of intermediate energy protons from states with surface peaked transition densities over a wide range of target masses and incident proton energies. At the present time it is not known why the low energy pion measurements<sup>31</sup> yield hadronic deformation lengths which for the 1.78 MeV  $2^+$  state are higher than the average of the proton results.

The giant resonance region which extends from about 16–25 MeV of excitation energy was found to be highly

TABLE III. Sum rule depletion for the ISGQR in  $^{28}\text{Si}$ .

$E_x$ (MeV)	EWSR (%) 250 MeV p	EWSR (%) 115 MeV p <sup>a</sup>	EWSR (%) 120 MeV $\alpha^b$	EWSR (%) 129 MeV $\alpha^c$	EWSR (%) 155 MeV $\alpha^d$
16.0 <sup>-</sup>	4.0		2.2	2.98	
16.87					
16.87 <sup>-</sup>	2.5		2.2	2.90	
17.46					
17.46 <sup>-</sup>	6.5		3.3	3.44	
18.48					
18.48 <sup>-</sup>	6.5	3	6.5	9.7	
19.44					
19.44 <sup>-</sup>	3.0		1.9	3.84	
20.30					
20.30 <sup>-</sup>	2.3		3.9	5.9	
21.0					
21.06 <sup>-</sup>	3.5		3.2	3.1	
22.64					
22.64 <sup>-</sup>	0.9		0.8	1.63	
23.52					
23.52 <sup>-</sup>	0.9		2.7		
25.0					
16.06 <sup>-</sup>	26	19 <sup>e</sup>	24.0 <sup>f</sup>	34.12 <sup>g</sup>	31 <sup>h</sup>
25.0					

<sup>a</sup>Reference 5.

<sup>b</sup>Reference 16.

<sup>c</sup>Reference 17.

<sup>d</sup>Reference 43.

<sup>e</sup>Summed region 15.7–24.1 MeV.

<sup>f</sup>Summed region 15.9–22.8 MeV.

<sup>g</sup>Summed region 15.3–24.7 MeV.

<sup>h</sup>Summed region 16.9–24.8 MeV.



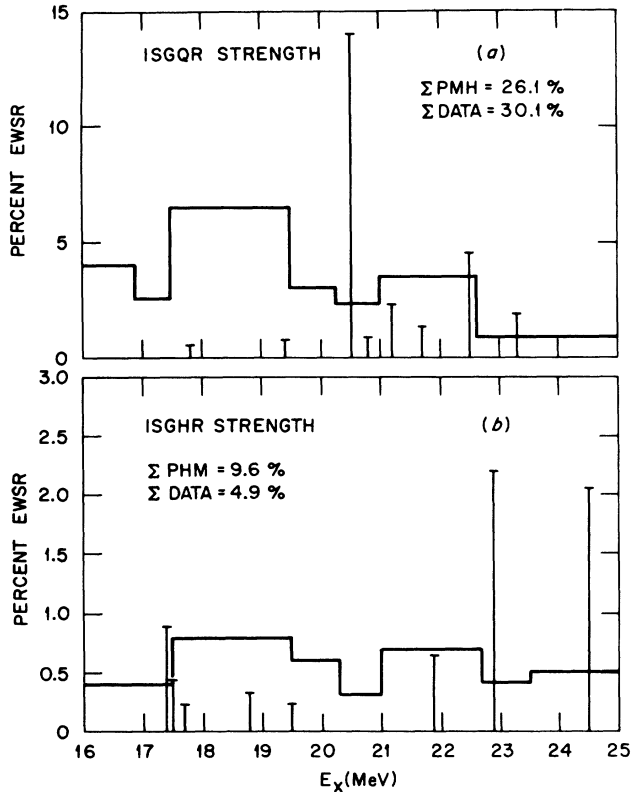


FIG. 10. Energy weighted sum rule depletions as measured in the present experiment (histogram) compared to the calculations (vertical lines) of Ref. 42 for the giant resonance region of 16–25 MeV. Part (a) is for the isoscalar giant quadrupole resonance (ISGQR), while part (b) is for the isoscalar giant hexadecapole resonance (ISGHR).

structured, in agreement with previous work. The integrated cross section for the region of excitation from 16 to 25 MeV shows the presence of  $L = 1, 2,$  and 4 multipoles, with sum rule fractions of 70 (adopted from photonuclear studies<sup>40</sup>), 26, and 5%, respectively. In normalizing the shape of the photonuclear data to match the 6 deg data at 19.5 MeV, and including the contribution of the ISGQR the proton spectral shape could be fairly well reproduced for excitation energies higher than 19.5 MeV. This allowed us to determine an upper limit of 4.5 MeV for the isovector potential  $V_{\tau}$ . For excitation energies below 19.5 MeV, the cross section is much higher than the addition of the IVGDR and ISGQR strengths. This we attribute to the excitation of  $M1$  and isovector spin-flip dipole strength. The sum rule exhaustion for the ISGQR is in

agreement both in magnitude and distribution with previous proton and alpha particle results as shown in Table III.

Schmid has calculated<sup>44</sup> the distribution of multipole strength in the giant resonance region using a microscopic angular momentum projected deformed particle hole model (PHM). The results of these calculations along with our data for the ISGQR and ISGHR are shown in Fig. 10. The calculated EWSR depletion<sup>44</sup> for the ISGQR agrees very well with the present results. However, the distribution of the strength is different. Our data shows an ISGHR strength of 5% EWSR for the 16–25 MeV region, while the PHM predicts 9.6% over this same energy interval. The distribution of ISGHR strength is shown in Fig. 10(b). In the PHM most of the EWSR strength for the ISGHR (22.5%) is found in the vicinity of 26 MeV. We see no structure near the 26 MeV region. The authors of the 115 MeV proton experiment deduced on EWSR depletion for the ISGHR of 8% over the GR region of 16–25 MeV. Schmid calculates for the GR region a sum rule of 4.1% for the ISGMR. We would not be sensitive to this strength. The PHM calculations give an ISGQR strength in the region of 16–24 MeV of 11% of the sum rule. We have not included any  $L = 3$  strength in our analysis since it was not needed in order to fit the angular distributions of Figs. 7 and 8 and ISGQR strength was not seen in earlier ( $\alpha, \alpha'$ ) (Ref. 16) and ( $p, p'$ ) (Ref. 5) studies.

In agreement with previous work, we find no evidence for any structures above 25 MeV up to our experimental limit of 45 MeV. The PHM predicts significant strength for  $L = 0, 1, 2, 3,$  and 4 excitations in this energy region, with sum rule depletions of 27% for the ISGMR, 30% for the IVGDR, 19% for the ISGQR, 19% for the ISGOR, and 55% for the ISGHR. In most cases the strength is spread out over this region, making it experimentally difficult to observe.

#### ACKNOWLEDGMENTS

We would like to thank TRIUMF staff members Dr. C. A. Miller, Dr. R. Abegg, and Dr. D. A. Hutcheon for their assistance in operating the MRS. Useful discussions on quasifree scattering with Dr. M. J. Iqbal were most helpful. The Oak Ridge National Laboratory participants were supported by Martin Marietta Energy Systems, Inc. under Contract No. DE-AC05-84OR21400 with the U.S. Department of Energy. The University of Oregon and Oregon State University participants were supported in part by grants from the National Science Foundation.

\*Also at Joint Institute for Heavy Ion Research, Oak Ridge, TN 37831.

<sup>1</sup>N. Marty, M. Morlet, A. Willis, V. Comparat, and R. Frascaria, Nucl. Phys. **A238**, 93 (1975).

<sup>2</sup>T. A. Carey, W. D. Cornelius, N. J. DiGiacomo, J. M. Moss, G. S. Adams, J. B. McClelland, G. Pauletta, C. Whitten, M.

Gazzaly, N. Hintz, and C. Glashauser, Phys. Rev. Lett. **45**, 239 (1980).

<sup>3</sup>F. E. Bertrand, E. E. Gross, D. J. Horen, J. R. Wu, J. Tinsley, D. K. McDaniels, L. W. Swenson, and R. Liljestrand, Phys. Lett. **103B**, 326 (1980).

<sup>4</sup>C. Djalali, N. Marty, M. Morlet, and A. Willis, Nucl. Phys.

- A380, 42 (1982).
- <sup>5</sup>S. Kailas, P. P. Singh, A. D. Bacher, C. C. Foster, D. L. Friesel, P. Schwandt, and J. Wiggins, *Phys. Rev. C* **25**, 1263 (1982).
- <sup>6</sup>J. R. Tinsley, D. K. McDaniels, J. Lisantti, L. W. Swenson, R. Liljestrand, D. M. Drake, F. E. Bertrand, E. E. Gross, D. J. Horen, and T. P. Sjoreen, *Phys. Rev. C* **28**, 1417 (1983).
- <sup>7</sup>S. Kailas, P. P. Singh, D. L. Friesel, C. C. Foster, P. Schwandt, and J. Wiggins, *Phys. Rev. C* **29**, 2075 (1984).
- <sup>8</sup>D. K. McDaniels, J. R. Tinsley, J. Lisantti, D. M. Drake, I. Bergqvist, L. W. Swenson, F. E. Bertrand, E. E. Gross, D. J. Horen, T. P. Sjoreen, R. Liljestrand, and H. Wilson, *Phys. Rev. C* **33**, 1943 (1986).
- <sup>9</sup>G. S. Adams, T. A. Carey, J. B. McClelland, J. M. Moss, S. J. Seestrom-Morris, and D. Cook, *Phys. Rev. C* **33**, 2054 (1986).
- <sup>10</sup>F. E. Bertrand, E. E. Gross, D. J. Horen, R. O. Sayer, T. P. Sjoreen, D. K. McDaniels, J. Lisantti, J. R. Tinsley, L. W. Swenson, J. B. McClelland, T. A. Carey, K. Jones, and S. J. Seestrom-Morris, *Phys. Rev. C* **34**, 45 (1986).
- <sup>11</sup>G. R. Satchler, *Nucl. Phys.* **A195**, 1 (1972).
- <sup>12</sup>F. E. Bertrand, D. C. Kocher, E. E. Gross and E. Newman, Oak Ridge National Laboratory Report No. 5137, 1975 (unpublished), p. 63.
- <sup>13</sup>K. Van der Borg, M. N. Harakeh, A. Van der Woude, and F. E. Bertrand, *Nucl. Phys.* **A341**, 219 (1980).
- <sup>14</sup>J. L. Ullmann, F. P. Brady, D. H. Fitzgerald, G. A. Needham, J. L. Romero, C. M. Castaneda, and N. S. P. King, *Nucl. Phys.* **A386**, 179 (1982).
- <sup>15</sup>D. H. Youngblood, P. Bogucki, J. D. Bronson, V. Garg, Y-W. Lui, and C. M. Rozsa, *Phys. Rev. C* **23**, 1997 (1981).
- <sup>16</sup>K. Van der Borg, M. N. Harakeh, and A. Van der Woude, *Nucl. Phys.* **A365**, 243 (1981).
- <sup>17</sup>Y. W. Lui, J. D. Bronson, D. H. Youngblood, Y. Toba, and U. Garg, *Phys. Rev. C* **31**, 1643 (1985).
- <sup>18</sup>D. K. McDaniels, J. Lisantti, J. Tinsley, I. Bergqvist, L. W. Swenson, F. E. Bertrand, E. E. Gross, and D. J. Horen, *Phys. Lett.* **162B**, 277 (1985).
- <sup>19</sup>D. K. McDaniels, J. Lisantti, I. Bergqvist, L. W. Swenson, X. Y. Chen, D. J. Horen, F. E. Bertrand, E. E. Gross, C. Glover, R. Sayer, B. L. Burks, O. Häusser, and K. Hicks, *Nucl. Phys.* **A467**, 557 (1987).
- <sup>20</sup>D. J. Horen, F. E. Bertrand, E. E. Gross, T. P. Sjoreen, D. K. McDaniels, J. R. Tinsley, J. Lisantti, L. W. Swenson, J. B. McClelland, T. A. Carey, S. J. Seestrom-Morris, and K. Jones, *Phys. Rev. C* **30**, 709 (1984).
- <sup>21</sup>K. W. Jones, C. Glashauser, R. de Swiniarski, S. Nanda, T. A. Carey, W. Cornelius, J. M. Moss, J. B. McClelland, J. R. Comfort, J. L. Escudie, M. Gazzaly, N. Hintz, G. Igo, M. Haji-Saeid, and C. A. Whitten, Jr., *Phys. Rev. C* **33**, 17 (1986).
- <sup>22</sup>R. P. Liljestrand, G. S. Blanpied, W. R. Coker, C. Harvey, G. W. Hoffmann, L. Ray, C. Glashauser, G. S. Adams, T. S. Bauer, G. Igo, G. Pauletta, C. A. Whitten, Jr., M. A. Oothoudt, B. E. Wood, and H. Nann, *Phys. Rev. Lett.* **42**, 363 (1979).
- <sup>23</sup>A. M. Bernstein, V. R. Brown, and V. A. Madsen, *Comments Nucl. Part. Phys.* **11**, 203 (1983).
- <sup>24</sup>TRIUMF experiments 272 and 335, also K. Lin, M. S. thesis, Simon Fraser University (1987), unpublished.
- <sup>25</sup>SAID, R. A. Arndt (unpublished).
- <sup>26</sup>J. Raynal, private communications.
- <sup>27</sup>S. W. Brain, A. Johnstons, W. A. Gillespie, E. W. Lees, and R. P. Singhal, *J. Phys. (London)* **G 3**, 821 (1977).
- <sup>28</sup>40 MeV: R. De Leo, G. D'Erasmus, A. Pantaelo, G. Pasquariello, G. Viesti, M. Pignanelli, and H. V. Geramb, *Phys. Rev. C* **19**, 646 (1979). 65 MeV: S. Kato, K. Okada, M. Kondo, K. Hosono, T. Saito, N. Matsuoka, K. Hatanaka, T. Noro, S. Nagamachi, H. Shimizu, K. Ogino, Y. Kadota, S. Matsuki, and M. Wakai, *ibid.* **31**, 1616 (1985). 115 MeV: Ref. 5. 135 MeV: Stan Yen, private communication. 200, 250, and 400 MeV: Ref. 24. 500 MeV: Dave Cook, private communication.
- <sup>29</sup>C. W. De Jager, H. DeVries, and C. DeVries, *At. Data Nucl. Data Tables* **14**, 479 (1974).
- <sup>30</sup>C. Olmer, D. F. Geesaman, B. Zeidman, S. Chakravarti, T. S. H. Lee, R. L. Boudrie, R. H. Siemssen, J. F. Amann, C. L. Morris, H. A. Thiessen, G. R. Bureson, M. J. Devereux, R. E. Segel, and L. W. Swenson, *Phys. Rev. C* **21**, 254 (1980).
- <sup>31</sup>U. Wienands, N. Hessey, B. M. Barnett, F. M. Rozon, H. W. Roser, A. Altman, R. R. Johnson, D. R. Gill, G. R. Smith, C. A. Wiedner, D. M. Manley, B. L. Berman, H. J. Crawford, and N. Grion, *Phys. Rev. C* **35**, 708 (1987).
- <sup>32</sup>D. S. Gale and J. S. Eck, *Phys. Rev. C* **7**, 1950 (1973).
- <sup>33</sup>F. E. Bertrand, *Nucl. Phys.* **A354**, 129c (1981).
- <sup>34</sup>J. Lisantti, J. R. Tinsley, D. M. Drake, I. Bergqvist, L. W. Swenson, D. K. McDaniels, F. E. Bertrand, E. E. Gross, D. J. Horen, and T. P. Sjoreen, *Phys. Lett.* **147B**, 23 (1984).
- <sup>35</sup>J. W. Watson, P. J. Pella, B. D. Anderson, A. R. Baldwin, T. Chitrakorn, C. C. Foster, and I. J. Van Heerden, *Phys. Lett. B* **181**, 47 (1986).
- <sup>36</sup>A. Brockstedt, B. Jakobson, and I. Bergqvist, private communication.
- <sup>37</sup>G. F. Bertsch and O. Scholten, *Phys. Rev. C* **25**, 804 (1982); H. Esbensen and G. F. Bertsch, *Ann. Phys. (NY)* **157**, 255 (1984); H. Esbensen and G. F. Bertsch, *Phys. Rev. C* **34**, 1419 (1986). Calculations were performed using the program SURF as provided by H. Esbensen.
- <sup>38</sup>L. W. Swenson, X. Y. Chen, J. Lisantti, D. K. McDaniels, I. Bergqvist, F. E. Bertrand, D. J. Horen, E. E. Gross, C. W. Glover, R. Sayer, B. L. Burks, O. Häusser, K. Hicks, and M. J. Iqbal, submitted to *Phys. Rev. C*.
- <sup>39</sup>C. J. Horowitz and M. J. Iqbal, *Phys. Rev. C* **33**, 2059 (1986). All calculations were performed using PWIA as provided by J. Iqbal.
- <sup>40</sup>J. Ahrens, H. Borchert, K. H. Czock, H. B. Eppler, H. Gimm, H. Gundrum, M. Kröning, P. Riehn, G. Sita Ram, A. Ziegler, and B. Ziegler, *Nucl. Phys.* **A251**, 479 (1975).
- <sup>41</sup>D. J. Horen, J. Lisantti, R. L. Auble, F. E. Bertrand, B. L. Burks, E. E. Gross, R. O. Sayer, D. K. McDaniels, K. W. Jones, J. B. McClelland, S. J. Seestrom-Morris, and L. W. Swenson, submitted to *Phys. Rev. C*.
- <sup>42</sup>R. Sawafta, O. Häusser, R. Abegg, W. P. Alford, R. Henderson, K. Hicks, K. P. Jackson, J. Lisantti, C. A. Miller, M. C. Vetterli, and S. Yen, *Phys. Lett. B* **201**, 219 (1988).
- <sup>43</sup>K. T. Knöpfle, G. J. Wagner, A. Kiss, M. Rogge, C. Mayer-Borricke, and Th. Bauer, *Phys. Lett.* **64B**, 263 (1976).
- <sup>44</sup>K. W. Schmid, *Phys. Rev. C* **24**, 1283 (1981).